Engineered Science
DOI: https://dx.doi.org/10.30919/es1193

Simulation Effect of Laser Moving Speed and Spot Size on Maximum Temperature in Laser Welding Human Skin Tissue

Totsaphon Chabuanoi,[1] Nattadon Pannucharoenwong[1,*] Phanuwat Wongsangnoi[2,*] Phadungsak Rattanadecho,[1] Jedsadakorn Saemathong[1], Suwipong Hemathulin[2] and Suphasit Panvichien[3]

Abstract

This paper presents a study focused on the development of computer simulation. The research involves the application of a moving laser onto a three-dimensional model of human skin tissue, which comprises three layers. This study focuses on how the speed of the laser moving and the spot size of the laser beam affect the maximum temperature after welding biological tissues. The critical point of concern is when the temperature exceeds 65 °C, as this level of heat can lead to damage to the skin tissue. The results of the study showed that when changing the speed of the laser moving from 50 mm/s to 250 mm/s in increments of 50 mm/s, the maximum average temperature after tissue welding with the laser was found to be 63 °C, 67.1 °C, 70.7 °C, 70.1 °C, and 70.9 °C, respectively. Similarly, altering the laser radius from 0.1 mm to 0.5 mm in increments of 0.1 mm. The average temperatures after biological tissue welding of 71.4 °C, 69.4 °C, 62.9 °C, 55.7 °C and 52 °C respectively. A larger radius of the laser spot results in a lower maximum temperature. Comparison with previous tissue studies revealed similar trends in temperature curves. The findings of this study can be further explored in the future by changing the laser's movement patterns to reduce the impact of thermal induced damage.

Keywords: Laser moving; Mathematical models; Laser welding skin tissue; Beer Lambert equation; Laser bioheat.
Received: 03 February 2024; Revised: 19 June 2024; Accepted: 07 July 2024.
Article type: Research article.

1. Introduction

Treating a wound involves letting the tissues of an organ to fuse at the cellular level by generating proteins that fortify the wound. However, excessive protein production can lead to larger scars. There are various methods for wound closure, such as stitches or using adhesive tapes, but these techniques can increase tissue inflammation, delaying the healing process. This can cause distress to patients and result in larger scars, which may not be suitable for certain cases that require rapid wound healing, reduced infection risk, minimal inflammation, and smaller scars. The examples include treating battlefield injuries, post-surgical wound care, and managing wounds resulting from surgeries.

Laser welding is a promising alternative to traditional suturing for wound closure. It offers several advantages, including reduced healing time, less inflammation, minimal scarring, and the ability to treat areas that are difficult to access. In recent years, several studies have investigated different laser welding techniques for wound healing. In 2019, Cong Li *et al.*[1] used a Nd:YAG fiber laser to weld porcine skin samples coated with BSA. Porcine skin is similar to human skin in terms of its structure and optical properties. The test specimens were 30x20x2 mm in size and were immersed in saline solution to increase light absorption. Three different laser scanning patterns were tested: segmentation, continuous wave, and pulsed. The results showed that the segmentation pattern produced the strongest welds. In 2020, Jun Huanh *et al.*[2] investigated four different laser scanning patterns: toothed path, circle path, Peane path, and heartbeat path. The results showed that the Peane path pattern produced the most uniform welds with minimal thermal damage. In 2020, Cong Li and colleagues determined suitable parameters by setting damage thresholds to 1 using the Arrhenius equation.[3] They tested these parameters by laser welding actual wounds and compared the results. Their calculations yielded parameters:

[1] *Department of Mechanical Engineering, Faculty of Engineering, Thammasat School of Engineering, Thammasat University, 12120, Thailand.*
[2] *Department of Mechanical and Industrial, Faculty of Industrial Technology, Sakon Nakhon Rajabhat University, 47000, Thailand.*
[3] *School of Biomedical Engineering & Imaging Sciences, Faculty of Life Sciences & Medicine King's College London, WC2R 2LS, United Kingdom.*
**Email:* pnattado@engr.tu.ac.th (N. Pannucharoenwong), wongsangnoi@hotmail.com (P. Wongsangnoi)

Power = 2.502 watts, Speed = 150 mm/s, and Pulse = 150 Hz. They applied these parameters in repeated pigskin experiments ten times, observing an average damage threshold of 0.715. The experimental group using these calculated parameters showed more efficient bonding than the non-calculated group and avoided skin damage from heat. In 2021, Cong Li and Kehong Wang utilized pigskin coated with BSA for 20 minutes and exposed the wound to laser irradiation, recording temperature data.[4] They conducted tensile testing to measure weld strength and assessed protein values via Raman spectrum. The findings indicated that a 55 ℃ weld temperature was the most suitable for providing the highest weld strength. Additionally, as the temperature increased, the protein degradation rate accelerated. Moreover, there are many studies being conducted in laboratories investigating tissue welding using lasers.[5-10]

In addition to that, there are also experimental research studies conducted on laboratory animals that yield results reasonably close to human conditions. The wound healing techniques help wounds heal faster and reduce inflammation.[11-13] However, due to limitations in the number and cost of experiments, there is not yet a sufficiently diverse range of techniques in animal testing.

However, the previous studies mostly involved the experiments on the real tissue samples from living organisms, which required repetitive trials to determine the suitable parameters for treatment. This approach consumes time and budget for treatment experimentation. Creating heat model simulations for tissue is another approach to forecast treatment outcomes before actual treatment or testing on real tissue samples. This can help reduce the trial duration to find the suitable treatment parameters and enhance prediction accuracy for post-treatment tissue temperatures by laser irradiation. An optimal temperature should not exceed 65 ℃ as tissue damage occurs at higher temperatures while excessively low temperatures may hinder strong tissue bonding.

Currently, there're research papers focusing on creating models to study laser treatments on skin tissues in various diseases. For instance, in 2018, Patcharaporn Wongchadakul *et al.* conducted a study on modeling the effects of wavelength, laser irradiation intensity, and beam area on human skin tissue exposed to laser light. Their experiment revealed that a wavelength of 532 nanometers absorbed the highest laser energy. Moreover, higher laser irradiation intensity resulted in increased tissue temperature, and a smaller receiving laser area led to higher skin temperatures.[14] Additionally, the numerous studies explore laser treatments, primarily focusing on static laser irradiation or mobile laser experiments conducted in laboratory settings using animal tissue samples.[15-21] However, these studies may not entirely represent real human skin tissue responses due to the absence of blood circulation and differing initial tissue temperatures compared to human tissue. Applying previous research findings to create models simulating human skin tissue and predicting laser wound healing outcomes from models closely resembling human tissue could significantly streamline treatment planning processes.

The wounds occurring during actual treatments have varied characteristics and sizes. Increasing the laser radius to control the heat administered to the different wound sizes might affect the heat generated within the tissue being treated. Additionally, when treating wounds with a moving laser, adjustments in the speed of the laser movement are necessary to prevent excessive heat at specific points. However, the true nature of heat generation and heat distribution within the wound tissue and surrounding tissue has not been fully explained. Fig. 1 illustrates the heat generation process resulting from the tissue welding with a moving laser. It demonstrates how the tissue receives heat from the laser as it moves over the wound and tissue. Understanding the heat patterns as the speed and radius of the laser change is an aspect that requires further investigation.

This research involved creating a model of living tissue for laser wound welding based on the Pennes' Bioheat equation. The laser was projected onto the model of human tissue divided into three layers: epidermis, dermis, and hypodermis, as shown in Fig. 1. The wound was welded by moving the laser under the Beer-Lambert equation along the wound. The variations in speed (v) and laser light radius (σ) were made to validate the accuracy of the model. The maximum temperature values were compared with actual experimental results to confirm the accuracy of the model. The parameters used in the study are outlined in Table 1 and Table 2.

Table 1. Laser parameters.

Welding parameters	Symbols	values
Power	P	3.5 W
speed	v	50 mm/s, 100 mm/s, 150 mm/s, 200 mm/s, 250 mm/s
Spot size	σ	0.1 mm, 0.2 mm, 0.3 mm, 0.4 mm, 0.5 mm
Welding time	t	900 s

2. Mathematical model

The study investigates the temperature impact on the biological tissue of human skin subjected to heat from a moving laser. The mathematical model used in the study comprises the multiple layers of biological tissue. It considers variations in the speed and radius of the laser to assess the maximum temperature reached after tissue welding.

2.1 Dimension of the skin model

The epidermis is the skin that covers the top layer of the body. Consists of cells arranged in layers. It is constantly being rebuilt and deteriorated. The newly created layer is at the bottom next to the dermis and gradually moves up to replace the upper layer of cells until it reaches the top layer called keratin. Epidermis also has melanin cells mixed in, causing

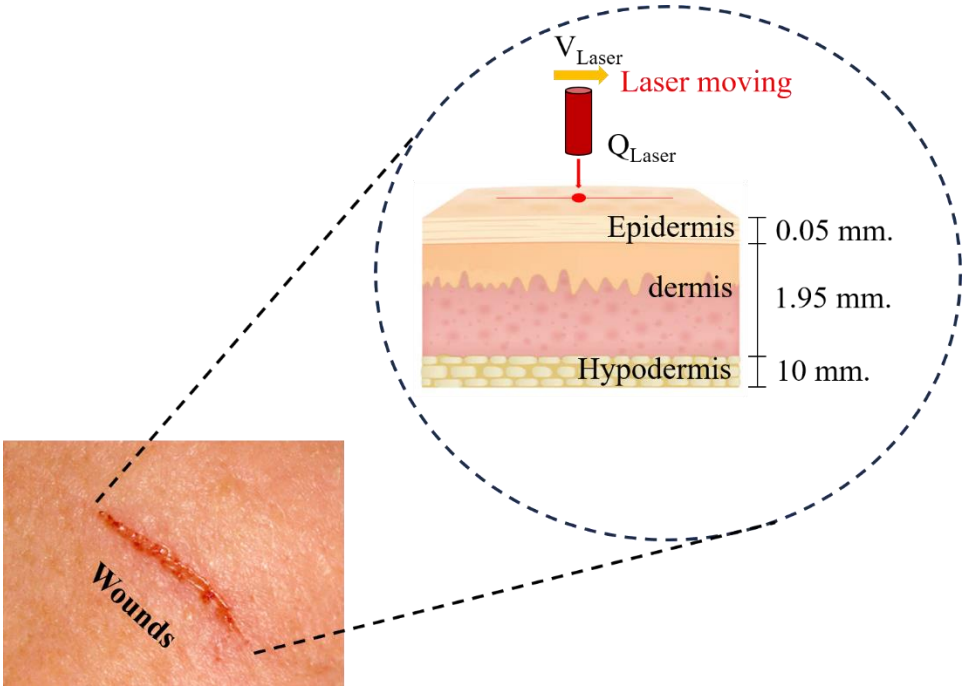

Fig. 1 Laser moving on the three layers of skin.

Table 2. Thermal properties, optical properties and physical properties.[22-27]

Properties	Symbols [Unit]	Epidermis	Demis	Hypodermis
Thickness	Z[mm]	0.05	1.95	10
Tissue	ρ [kg/m^3]	1,200	1,200	1,000
Specific heat of tissue	C_p [J/kg·K]	3,600	3,800	3,600
Thermal conductivity	K [W/ (m·K)]	0.21	0.53	0.55
Blood perfusion	w_b [1/s]	0	0.0031	0.0031
Absorption coefficient	α [1/m]	720	25.5	89
Scattering coefficient	β [1/m]	732	732	17,400
Ambient temperature	T_m [°C]	25		
Initial temperature	T_0 [°C]	37		
Blood temperature	T_b [°C]	37		
Heat convection coefficient	h [W/m^2·K]	20		
Blood density	ρ_b [kg/m^3]	1,060		
Specific heat of blood	C_b [J/kg·K]	3,660		

different skin colors. The dermis is the layer next to the epidermis. Consists of 2 types of tissue: 1. Collagen (collagen)serves to build strength and repair injured skin. If too much builds up, it causes scarring. 2. Elastic (elastic) acts on the flexibility of tissues. The dermis is the layer that has blood vessels, nerves, muscles, hair follicles, sebaceous glands, and sweat glands scattered throughout. The subcutaneous tissue or fat layer (Subcutaneous) is a layer that is mostly fat cells. The face warms the body and helps absorb external shocks. The three-dimensional model (3D) of skin tissue divided into three layers: epidermis, dermis, and hypodermis. Each layer has thicknesses of 0.05 mm, 1.95 mm, and 10 mm, respectively, based on the model dimensions proposed by P. Wongchadakul *et al.*[16] The layers are depicted as shown in Fig. 2, with each layer having a width of 20 mm along the Y-axis and a length of 30 mm along the X-axis, representing the path of the laser for wound welding.

2.2 Heat transfer analysis

The heat transfer within biological tissue occurs through two types of blood vessels: arteries and veins. The blood circulates in counter-current flow. The circulation of the blood vessel network through areas with varying environmental conditions and thermodynamics leads to differences in temperature between the blood vessels and the tissue they pass through. This results in the transfer of heat within the body, impacting the body's temperature regulation. The amount of heat transferred within the tissue depends on the varying rates of blood flow in different organs of the body.

In this study, the laser under investigation moves along the x-axis, emitting light onto the upper part of an epidermal layer model. The upper surface of tissue is convection of the surrounding air at a constant rate of 20 W/mm². The ambient temperature is 25 °C, and the initial temperature of the tissue is 37 °C, as shown in Fig. 3. The heat is transmitted through

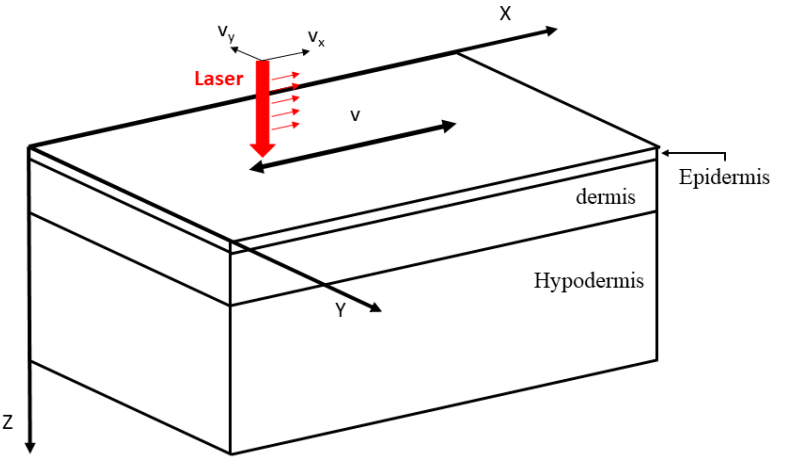

Fig. 2 Three-layer skin structure model with tissue welded using a laser moves in the x-direction.

each layer of the skin under the following assumptions:

1. The thermal properties and optical properties are constant.
2. There is no change in the state of the substance in the tissue.
3. There is no chemical reaction in the tissues.
4. Assumed a smooth continuity of the tissue surface.
5. Assumed tissue is homogeneous and isotropic.

The studies conducted have involved numerous models of heat transfer in living tissue. However, the widely used biological heat transfer model currently is the one proposed by Harry Pennes in 1948.[28] This model describes heat conduction and blood perfusion to maintain energy balance within the tissue, as represented in Equation (1).

$$\rho C \frac{\partial T}{\partial t} = K\nabla^2 T + \rho_b C_b \omega_b (T_a - T_b) + Q_{met} + Q_r \quad (1)$$

where ρ is density [kg/m^3], C the heat capacity of tissue [J/kg·°C], T the tissue temperature [°C], K the thermal conductivity [W/m·°C], Q_{met} the metabolic heat source within the tissue [W/m^2], Q_r the external heat source [W/m^2].

From an equation (1), according to Beer-Lambert law, the heat generation by a laser in tissue depends on the tissue's optical properties, such as absorption coefficient and scattering, light diffusion in tissue at depth z and radius r, as expressed in the equation.

$$I(Z) = I_0 e^{-\gamma z} \quad (2)$$

where $\gamma = \alpha+\beta$, I(Z) intensity in the z direction [W/m^2], I_0 intensity incident light [W/m^2], α the absorption coefficient[1/m], β the scattering coefficient[1/m], z the depth within the tissue [mm].

The heat energy generated in the tissue occurs solely from the accumulation of absorbed light within the tissue. The heat accumulation per area Q(r, z) within the thickness ∇z is expressed by Ref. [29-30].

$$Q(r,z) = \alpha I(r,z) \quad (3)$$

From an equation (2), let's assume that the absorption of heat energy occurs exclusively in the z-axis. The heat dispersion within the tissue originates from the heat generation source, represented as I(r, z), as described in equation (4).

$$I(r,z) = \alpha I_0 e^{\left(\frac{-r^2}{2\sigma(z)^2}\right)} e^{-\gamma z} \quad (4)$$

The σ is the width parameter of the Gaussian light distribution [mm]. If there's no light energy absorption (α=0), the energy at any depth z equals the energy emitted by the light source reaching the tissue.

$$P(z) = 2\pi I_0 \sigma^2(z) e^{-z\beta} \quad (5)$$

$$P(0) = 2\pi I_0 \sigma^2(0) \quad (6)$$

From an equation (4), where[31]

$$\sigma^2(z) = \sigma^2(0) e^{\beta z} \quad (7)$$

Replacing the equations (4) and (7) into (3), the energy equation is as follows:

$$Q(r,z) = \alpha I_0 e^{\left(\frac{-r^2}{2\sigma(0)^2}\right)} \cdot e^{\beta z} \cdot e^{-\gamma z} \quad (8)$$

From the energy equations for the heat source (6) and (8), when the heat source moves along the x-axis, the equation for the moving laser source can be written as per:[32,33]

$$Q(r,z) = \alpha \cdot \frac{P}{2\pi\sigma^2} \cdot e^{-\left(\frac{(x-vt)^2+y^2}{2\sigma^2}\right)} \cdot e^{\beta z} \cdot e^{-(\alpha+\beta)z} \quad (9)$$

where P is a constant Power of laser[W], v is laser moving velocity[mm/s].

The skin surface, there occurs heat convection between the skin and the air, with a constant heat transfer coefficient of 20 W/m².K, excluding sweat evaporation. The ambient temperature remains at 25 °C without considering heat loss through radiation. The study boundary can be represented as follows:

$$-n \cdot (-k\nabla T) = h_{am}(T - T_{am}) \quad (10)$$

where T_{am} is the ambient temperature [°C], h_{am} the ambient air heat transfer coefficient[W/m].

Assuming no resistance exists between the contact tissue layers, the internal boundaries are therefore assumed to be continuous boundary conditions,

$$n \cdot (k_u \nabla T_u - k_d \nabla T_d) = 0 \quad (11)$$

$$T_u = T_d \quad (12)$$

3. Method

This research constructed a three-dimensional skin tissue model and analyzed the heat equations using the Finite Element Method (FEM). The skin tissue model was created using COMSOL™ Multiphysics. The analysis of grid

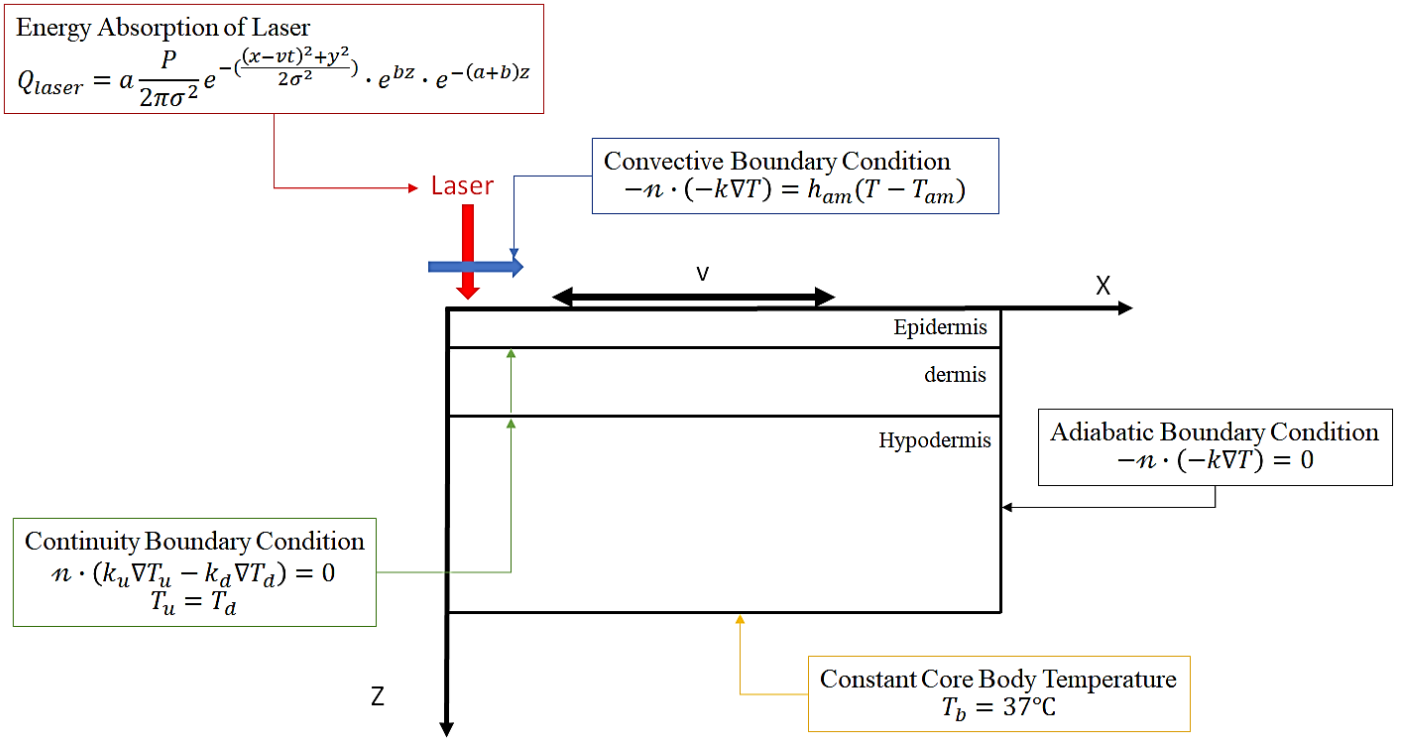

Fig. 3 Boundary condition and physical domain.

intensity to find the appropriate number of elements. Considering the analysis, approximately 80,000 elements were optimal (see Fig. 4). Adding more than this does not affect the accuracy of the model. The study investigated the changes in maximum heat when altering the laser's speed movement and the laser beam radius. The models were built by validating their accuracy based on previous research. Basic parameters of the skin were incorporated into the model, as listed in Tables 1 and 2.

The study varied the laser's speed from 50 mm/s. to 250 mm/s, increasing by 50 mm/s increments, while keeping the laser beam radius constant at 0.2 mm. It compared and contrasted the maximum temperatures in the skin tissue model. Then, using a fixed laser speed of 100 mm/s, the research altered the size of the laser beam from 0.1 mm to 0.5 mm in 0.1 mm increments. It compared the effects on the maximum temperature, aiming to identify the appropriate maximum temperature, which should not exceed 65 °C to prevent tissue damage and should not fall below 45 °C to ensure proper wound healing (see Fig. 5).

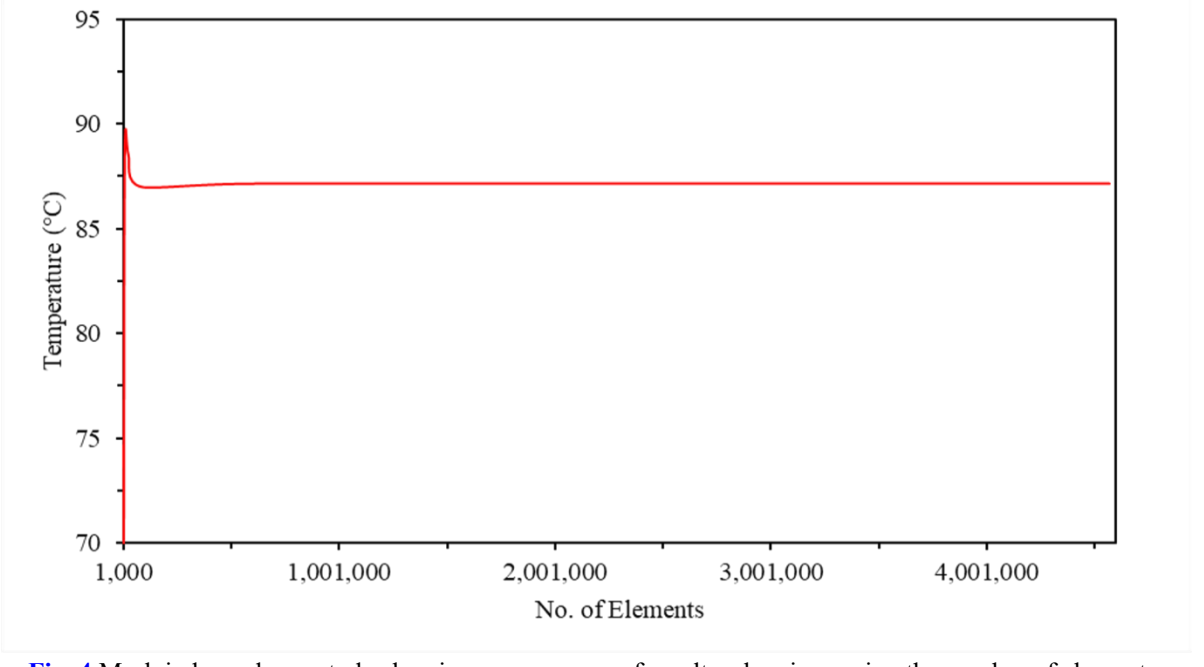

Fig. 4 Mesh independence study showing convergence of results when increasing the number of elements.

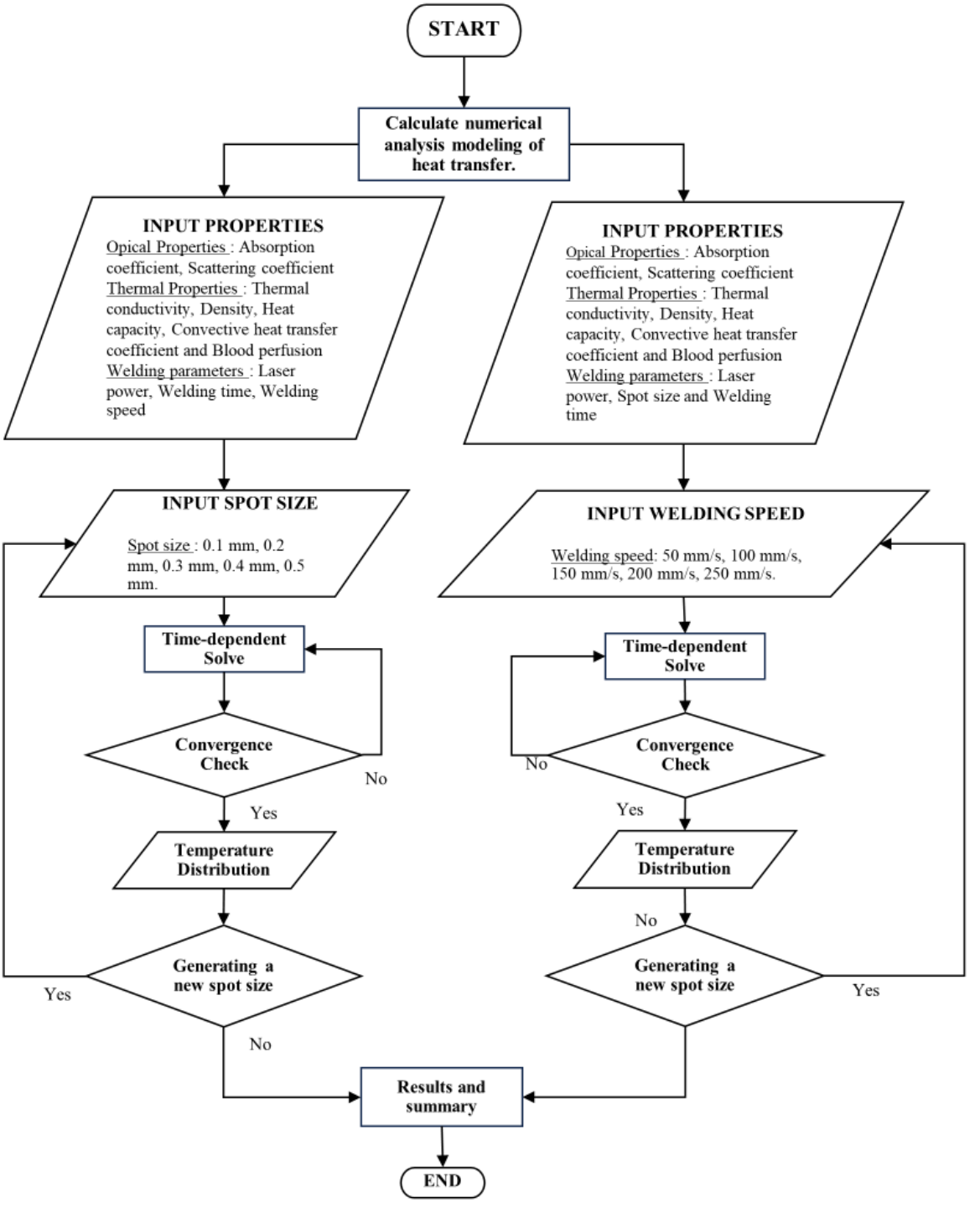

Fig. 5 The flow diagram of calculation laser welding skin tissue.

4. Verification

The verification of the model's accuracy was conducted by comparing it with the findings of J. Saemathong *et al.*,[34] who investigated laser treatment for skin diseases. While adjusting parameters equally, they did not manipulate the laser's movement. The results obtained were found to be comparable, as shown in Fig. 6 and Fig. 7.

5. Results and discussion

The study aimed to develop a multi-layered skin model, consisting of the epidermis, dermis, and hypodermis, using the Beer-Lambert law to calculate heat transfer in human skin tissue. Employing a laser power of 3.5 W, the maximum temperature after the study should not exceed 65 °C to prevent tissue damage due to heat. The experiment involved altering the laser's radius while maintaining a constant speed of 100 mm/s to examine the resulting changes in peak temperatures during laser exposure to the skin tissue. Subsequently, with a fixed light radius of 0.2 mm, they investigated by varying the laser's speed, comparing the respective maximum

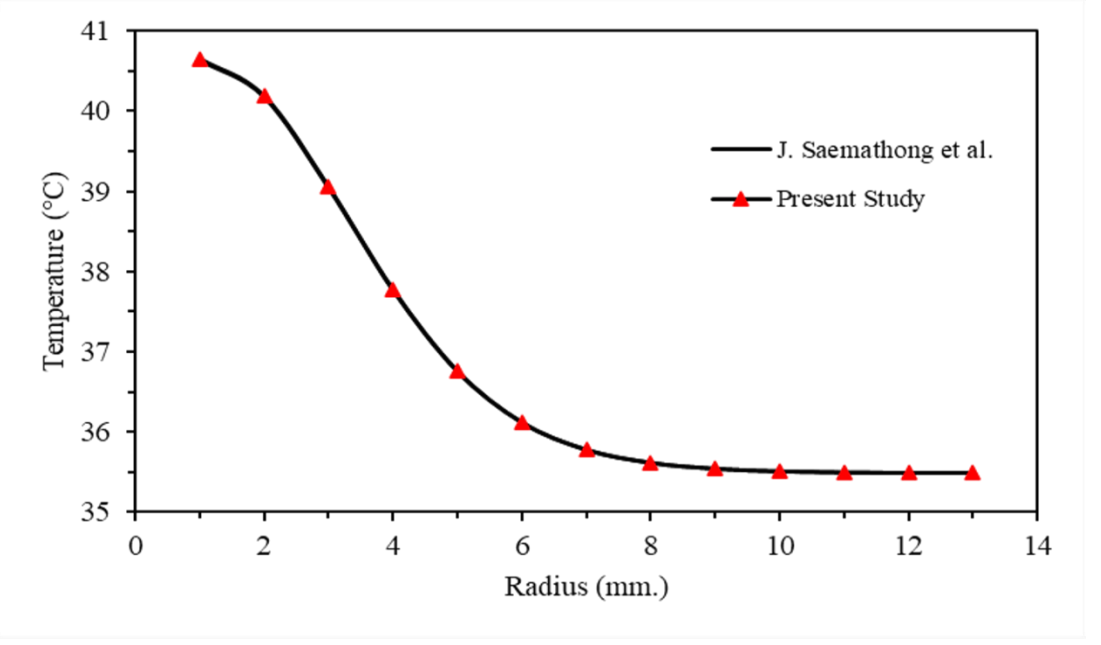

Fig. 6 Compare the radial tissue temperature distribution with the study of J. Saemathong *et al.*

temperatures reached.

In Fig. 8, at 200 seconds in top surface plane (Z= 0), it was observed that as the laser radius increased from 0.1 mm to 0.5 mm, the maximum temperatures recorded were 74.5 °C, 63.7 °C, 55.8 °C, 54.1 °C, and 50.6 °C, respectively. This study indicated a decrease in the maximum tissue temperature with an increase in the laser radius, while the temperature distribution increased with the increment of the laser radius. A smaller radius results in higher energy density of the laser emissions compared to a larger radius, thereby leading to a higher maximum temperature when the laser size is reduced. Additionally, increasing the size of the laser radius reduces the energy density and allows for greater energy dissipation.

Figure 9 presents the graph of the maximum temperature occurring during a 900-second laser irradiation study for wound welding. In Fig. 9(a), the average maximum temperature is approximately 74 ℃, with some segments of the study reaching temperatures as high as 135 ℃, leading to destruction of skin tissue due to the excessive heat exceeding 65 ℃. In Fig. 9(b), the average maximum temperature is around 70 ℃, with some parts of the study reaching up to 105 ℃, causing damage to skin tissue from temperatures surpassing 65 ℃. Fig. 9(c) depicts an average maximum temperature of about 60 ℃, with certain segments reaching up to 85 ℃, resulting in skin tissue damage due to temperatures exceeding 65 ℃. Fig. 9(d) shows an average maximum temperature of approximately 55 ℃, with certain portions reaching 70 ℃, leading to skin tissue damage from temperatures exceeding 65 ℃. In Fig. 9(e), the average maximum temperature is around 52 ℃, with some portions reaching 61 ℃, which remains within the suitable range below 65 ℃, preventing tissue damage due to excessive heat.

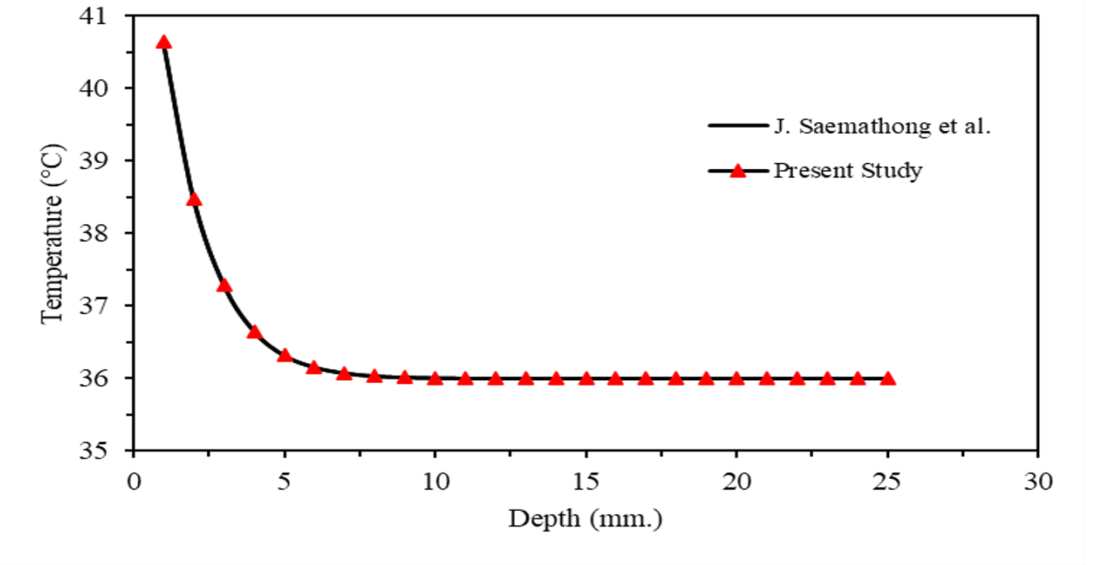

Fig. 7 Comparison of the depth temperature distribution with the study of J. Saemathong *et al.*

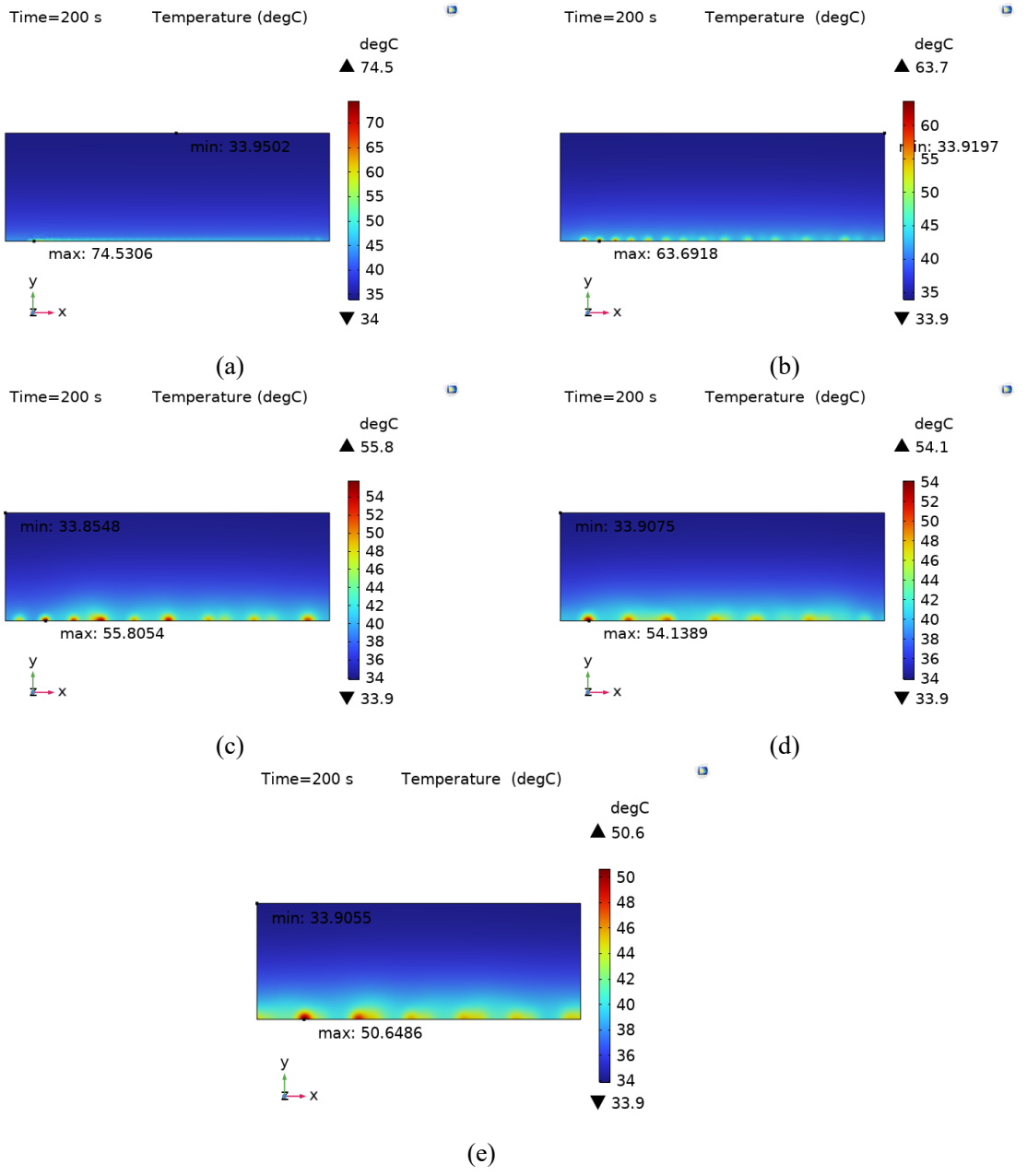

Fig. 8 Effect of laser radius on temperature distribution in top surface plane (Z= 0), increasing the laser radius leads to a more spread-out temperature distribution.; (a) 0.1 mm. (b) 0.2 mm. (c) 0.3 mm. (d) 0.4 mm. and (e) 0.5 mm.

Moreover, it's observed that increasing the laser radius narrows down the range of the maximum temperature, focusing it towards the optimum temperature line. This is caused by the effect of convection according to Equation (10). When the radius of the laser becomes larger, it causes energy dissipation and is carried by the outside air, causing the maximum temperature to decrease accordingly.

Figure 10 compares the average maximum temperature when increasing the laser radius. When increasing the size of the laser beam from 0.1 mm to 0.5 mm, the temperatures after tissue welding with the laser are 71.4 °C, 69.4 °C, 62.9 °C, 55.7 °C, and 52 °C, respectively. Notably, the lowest temperature is observed with a laser beam radius of 0.5 mm. It is evident from the graph that increasing the laser beam radius results in a reduction in the temperature after welding. This observation aligns with Equation (9), indicating that an increase in the laser beam radius leads to a decrease in the energy density, as the energy becomes less concentrated when the laser beam has a larger size.

Figure 11 displays the maximum temperature at 200 seconds in top surface plane (Z= 0), observed at different laser speeds from 50 mm/ 250 mm/s. The temperatures recorded are 61 °C, 64.4 °C, 86.5 °C, 67.8 °C, and 56.4 °C, respectively. According to the study, as the laser speed increases, the maximum tissue temperature also rises continuously until it reaches a speed of 150 mm/s. Then, it starts decreasing due to the change in the laser position as time progresses with the increased speed.

Figure 12 illustrates the graph of the maximum temperature recorded when altering the laser motion speed

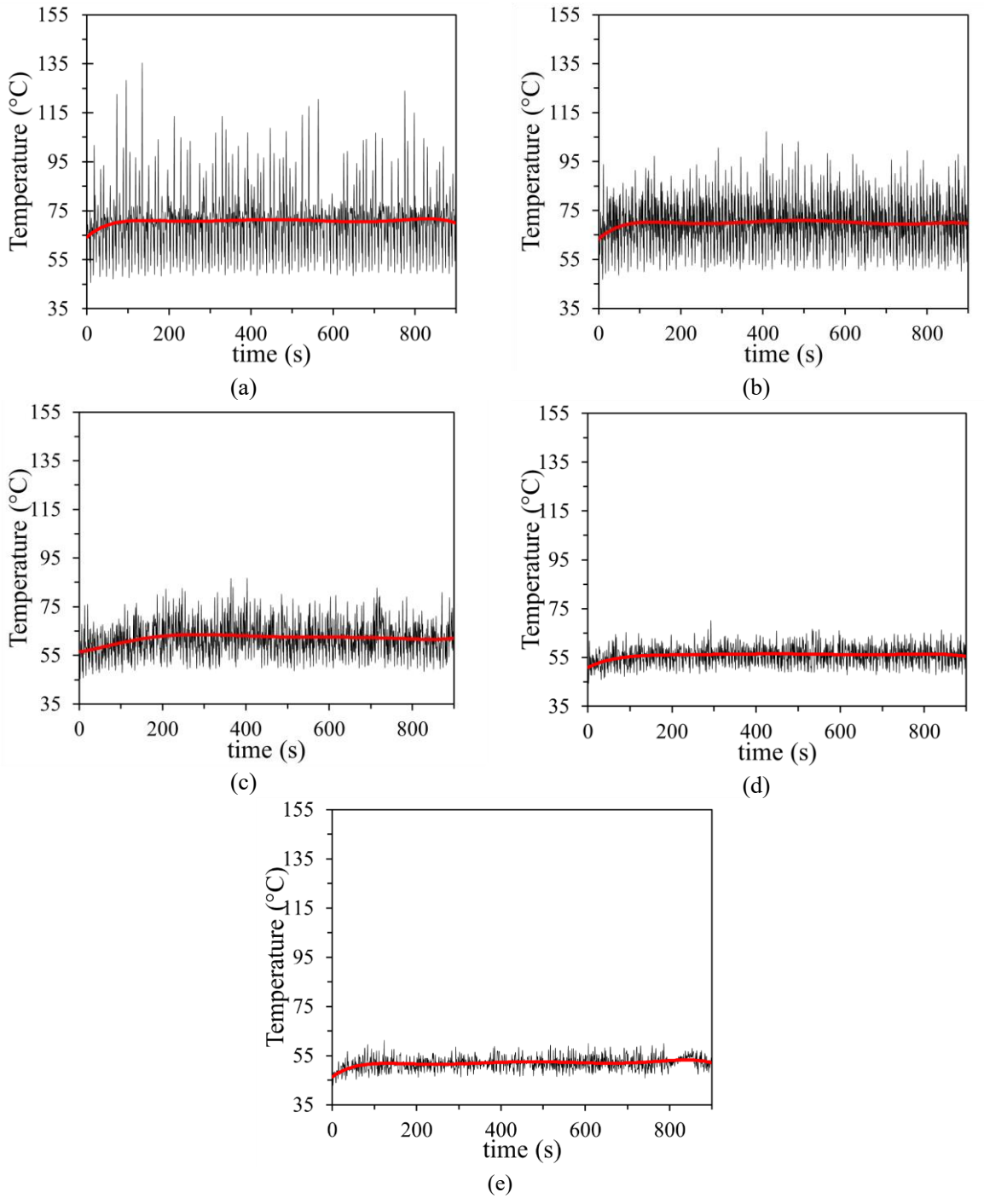

Fig. 9 The maximum temperature decreases with increasing laser radius. (a) 0.1 mm. (b) 0.2 mm. (c) 0.3 mm. (d) 0.4 mm. (e) 0.5 mm.

during a study of laser light exposure for wound healing over 900 seconds. In Fig. 12 (a), at a laser speed of 50 mm/s, the average maximum temperature reaches approximately 64 ℃, with some instances peaking at 110 ℃, causing tissue damage due to temperatures exceeding 65 ℃. In Fig. 12 (b), at 100 mm/s, the average maximum temperature is around 67 ℃, with occasional peaks at 98.9 ℃, slightly lower than at 50 mm/s but still causing tissue damage. Fig. 12 (c) depicts an average maximum temperature of 70 ℃ at a speed of 150 mm/s, occasionally reaching 99.9 ℃, causing slight tissue damage. In Fig. 12 (d), some peaks reach 95.4 ℃ at a similar temperature of around 70 ℃ at 150 mm/s causing excessive heat and tissue damage. Finally, in Fig. 12(e), there are moments where temperatures peak at 95.8 ℃ with an average maximum temperature of approximately 73 ℃. In addition, Fig.12 shows the range of maximum and minimum temperatures decreases as the laser speed increases. Fig.12(a)-Fig.12(e) the average difference between maximum and minimum temperatures is approximately 63 ℃, 51 ℃, 46 ℃, 41 ℃ and 25 ℃ respectively, which is a result of moving over the original location with increased speed, reducing the impact of heat loss from convection of outside air.

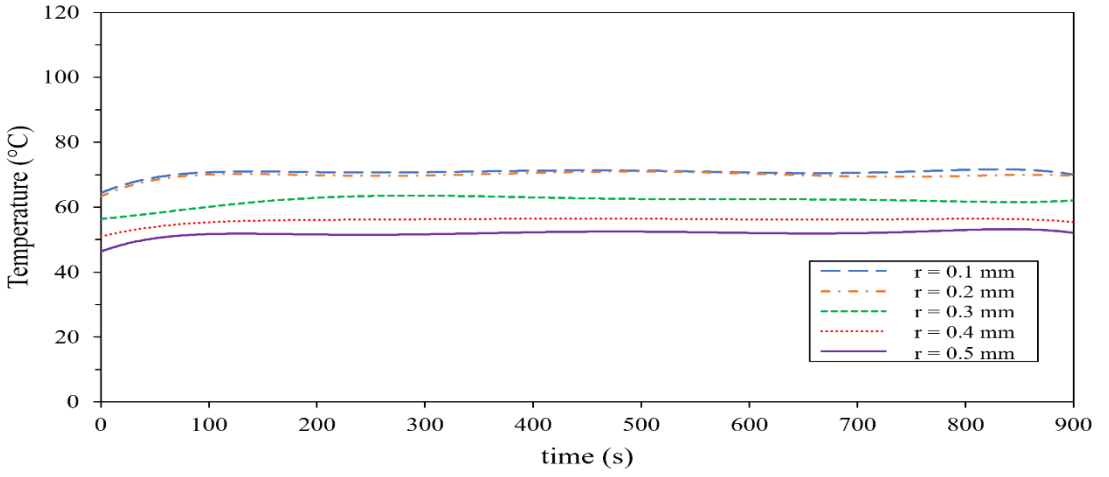

Fig. 10 Comparison of average peak temperature with varying laser radius: decreasing peak temperature with increasing radius.

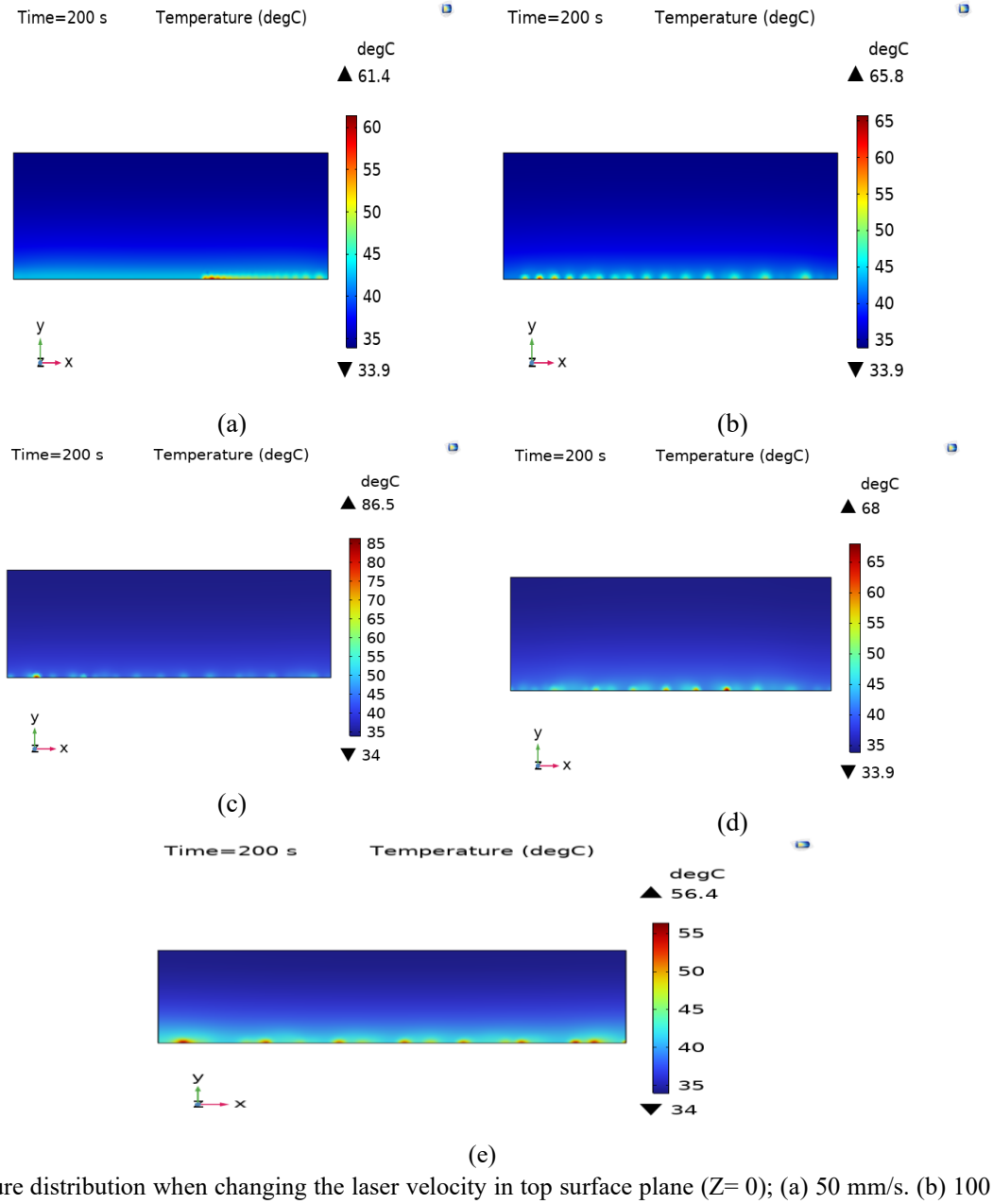

Fig. 11 Temperature distribution when changing the laser velocity in top surface plane (Z= 0); (a) 50 mm/s. (b) 100 mm/s. (C) 150 mm/s. (d) 200 mm/s. (e) 250 mm/s.

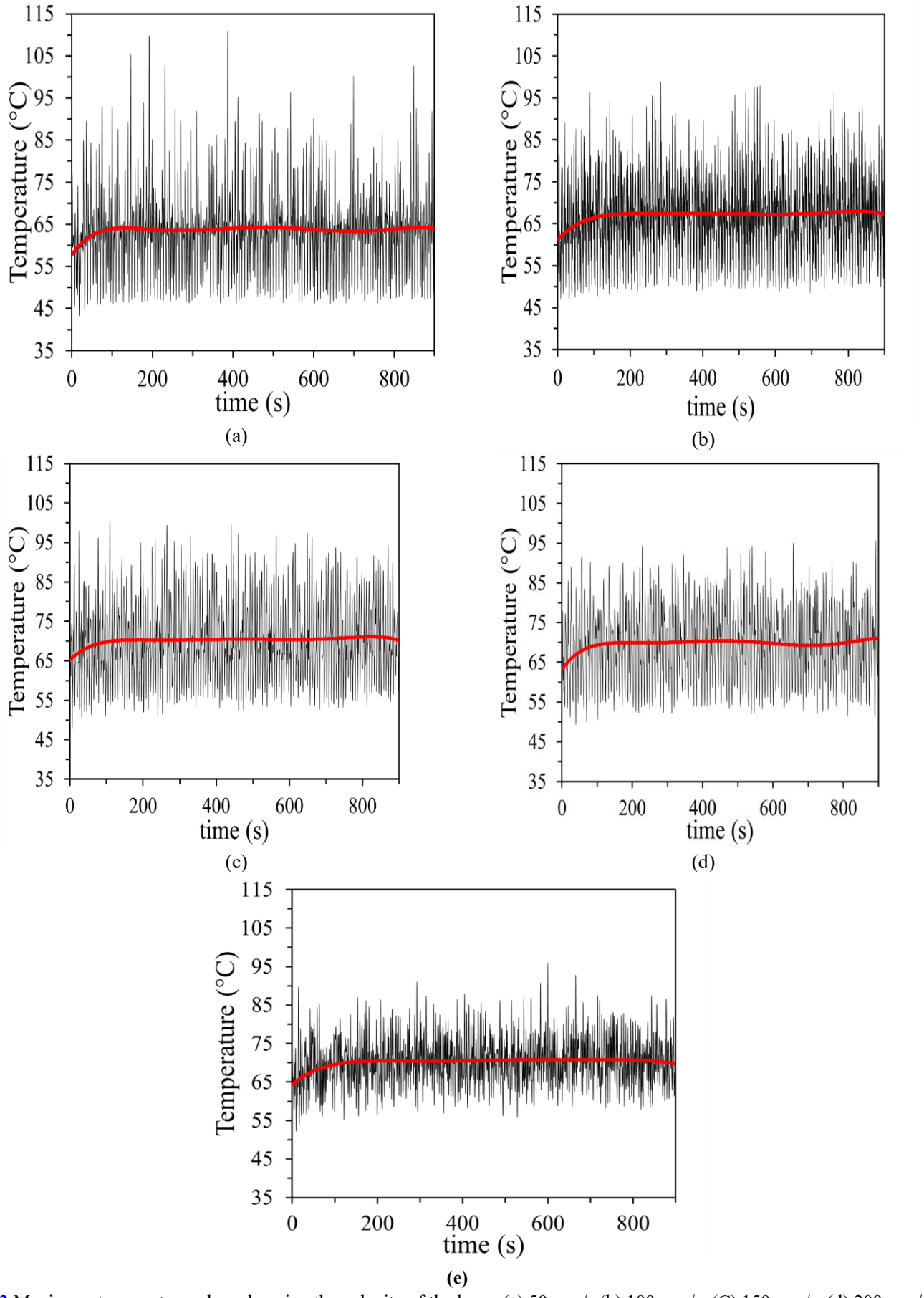

Fig. 12 Maximum temperature when changing the velocity of the laser; (a) 50 mm/s.(b) 100 mm/s. (C) 150 mm/s. (d) 200 mm/s. (e) 250 mm/s.

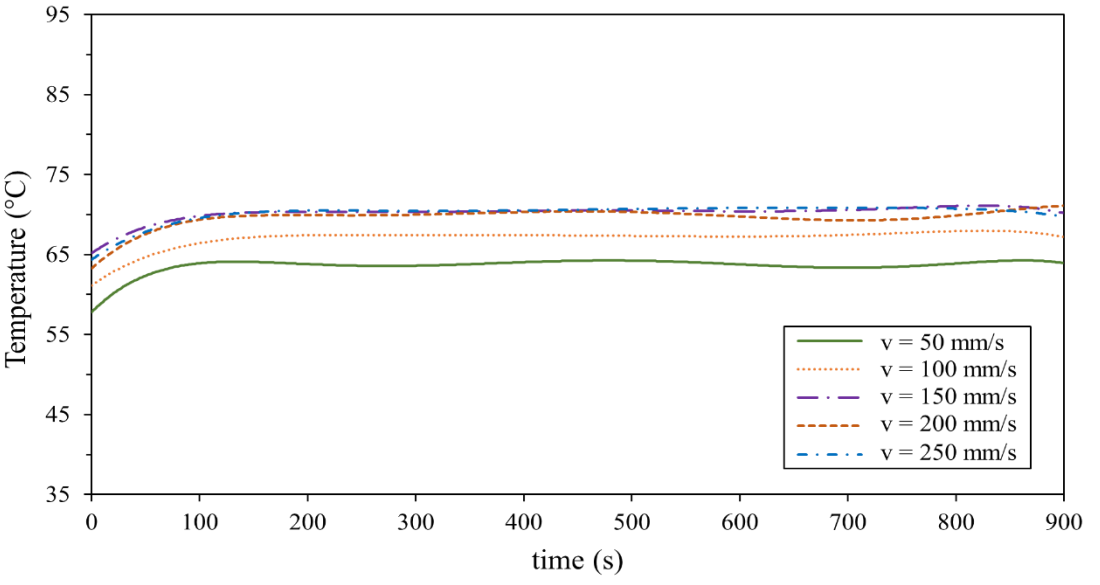

Fig. 13 compare the difference between the average maximum temperature when changing the laser velocity; when increasing the speed of the laser, it leads to an increase in the maximum temperature, which then gradually stabilizes.

Figure 13 illustrates the comparison of the maximum average temperature when changing the motion speed of the laser. When increasing the speed of laser motion to 50 mm/s, 100 mm/s, and 150 mm/s, the maximum average temperatures increase to 63 °C, 67.1 °C, and 70.7 °C, respectively. However, in the speed range of 200 mm/s to 250 mm/s, the average maximum temperatures are close to that at 150 mm/s. The temperatures after tissue welding are 70.1 °C and 70.9 °C, respectively. The increase in temperature with increased speed, followed by stabilization, is attributed to the absorption coefficient of the tissue. As the speed increases, the absorption coefficient leads to an increased absorption of heat energy from the moving laser. This is because the overlapping of the laser's original points of contact increases, resulting in the accumulation of heat energy, causing the maximum temperature to rise. However, when the speed reaches a certain value, the time for heat sensation from the laser decreases. The laser transmits heat to the skin surface, reducing the temperature gradually.

Figure 14 compares the results of modeling studies with the actual study by Cong Li *et al.* When the study results at a speed of 200 mm/s and a laser radius of 0.2 mm were compared, similarities in the graph's trends were observed. However, there were temperature ranges that differed due to initial temperatures, tissue properties, and varying blood flow rates.

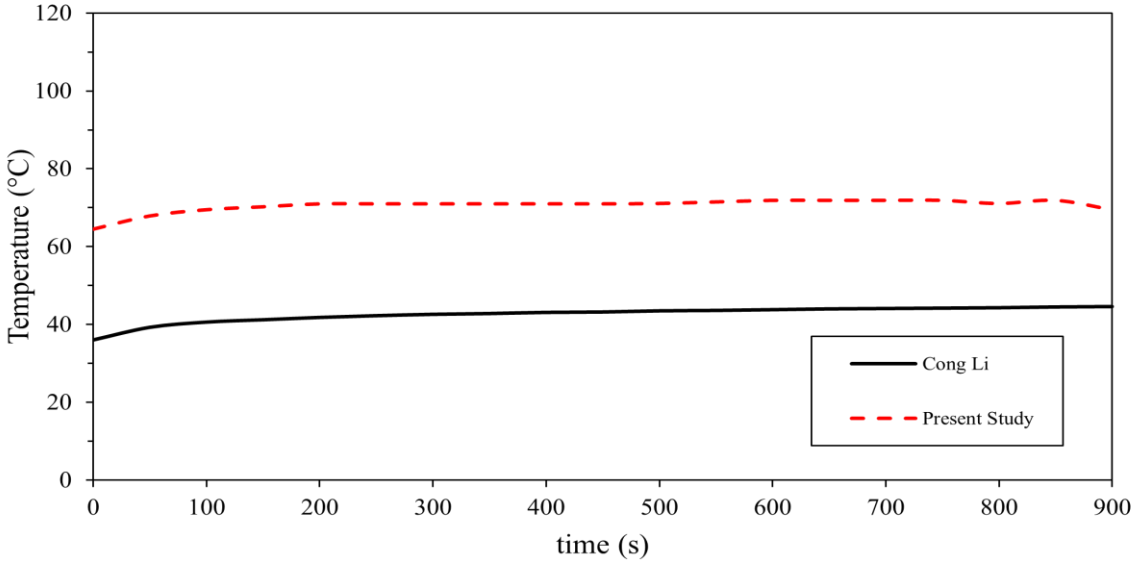

Fig. 14 Compare the temperature after tissue welding from the modeling study results with the study results by Cong Li *et al.* It was found that the trends of the temperature lines were similar but due to different initial temperatures, there were temperature differences.

6. Conclusion

The three-dimensional model study of human skin tissue, comprising the epidermis, dermis, and hypodermis layers, revealed varying thicknesses for each layer. When changing the laser radius from 0.1 mm to 0.5 mm while maintaining a constant laser motion speed, it resulted in an average reduction in the maximum tissue temperature. At a laser radius of 0.5 mm, the average maximum temperature was 52b °C, with the highest temperature reaching 61 °C, which did not exceed 65 °C. Consequently, the skin tissue remained undamaged by heat. Additionally, increasing the laser radius led to a narrower range between the maximum and minimum temperatures, tending more toward the average.

Furthermore, the effect of changing the moving speed of the laser used to weld the wound by increasing the laser speed in increments of 50 mm/s from 50 mm/s to 250 mm/s, with a constant laser radius of 0.2 mm. The findings indicated that as the laser speed increased, the average maximum tissue temperature rose consistently and remained stable from 150 mm/s to 250 mm/s. Moreover, accelerating the speed narrowed the range between the maximum and minimum temperatures, converging towards the average.

Due to this study, the laser's movement, which currently follows a straight line along the X-axis, can be further studied in the future by modifying its movement patterns into other forms. This could enhance temperature dispersion and reduce the impact of heat damage on tissue.

7. Significant of this work

This study is a study of numerical analysis modeling of heat transfer in three-layer thick biological tissues (epidermis, dermis, hypodermis) with laser welding. The study is based on the use of the biological heat equation and the laser moving equation. Previous research has not utilized laser motion equations for simulation purposes. The results help to understand the impact of relevant parameters to help reduce the side effects of excessive heat damage. The maximum temperature should not exceed 65 °C. The study was conducted to determine how changing the radius parameters of the laser and the speed of the laser affects the maximum temperature in laser welding. If this study proves to be successful, it will aid doctors in making more effective treatment plans.

Acknowledgments

This work was supported by the Thailand Science Research and Innovation Fundamental Fund fiscal year 2025, Graduate Studies Faculty of Engineering, Thammasat School of Engineering, Thammasat University Thailand and this study was supported by Thammasat University Research Fund, Contract No TUFT 35/2567.

Conflict of Interest

There is no conflict of interest.

Supporting Information

Not applicable.

References

[1] C. Li, K. Wang, J. Huang, Effect of scanning modes on the tensile strength and stability in laser skin welding *in vitro*, *Optik*, 2019, **179**, 408-412, doi: 10.1016/j.ijleo.2018.10.037.

[2] J. Huang, Y. Chen, Z. Chen, C. Li, K. Wang, Q. Zhou, Effects of scanning paths on laser welding, *Optics and Lasers in Engineering*, 2020, **130**, 106078, doi: 10.1016/j.optlaseng.2020.106078.

[3] C. Li, J. Huang, K. Wang, Q. Liu, Z. Chen, Investigation on thermal damage model of skin tissue *in vitro* by infrared laser welding, *Optics and Lasers in Engineering*, 2020, **124**, 105807, doi: 10.1016/j.optlaseng.2019.105807.

[4] C. Li, K. Wang, Effect of welding temperature and protein denaturation on strength of laser biological tissues welding, *Optics & Laser Technology*, 2021, **138**, 106862, doi: 10.1016/j.optlastec.2020.106862.

[5] D. Foyt, J. Johnson, R. Kirsch, J. Bruce, J. Wazen, Dural closure with laser tissue welding, *Otolaryngology - Head and Neck Surgery*, 1996, **115**, 513-518, doi: 10.1016/s0194-5998(96)70005-0.

[6] B. S. Bleier, M. A. Gratton, J. M. Leibowitz, J. N. Palmer, J. G. Newman, N. A. Cohen, Laser-welded endoscopic endoluminal repair of iatrogenic esophageal perforation: an animal model, *Otolaryngology–Head and Neck Surgery*, 2008, **139**, 713-717, doi: 10.1016/j.otohns.2008.08.006.

[7] B. S. Bleier, N. M. Cohen, J. D. Bloom, J. N. Palmer, N. A. Cohen, Laser tissue welding in lung and tracheobronchial repair, *Chest*, 2010, **138**, 345-349, doi: 10.1378/chest.09-2721.

[8] F. Xu, T. Wen, K. Seffen, T. Lu, Modeling of skin thermal pain: a preliminary study, *Applied Mathematics and Computation*, 2008, **205**, 37-46, doi: 10.1016/j.amc.2008.05.045.

[9] C. Li, K. Wang, J. Huang, J. Fan, Effects of dyes on tensile strength and thermal damage of laser biological tissue soldering, *Optik*, 2021, 227, 165945, doi: 10.1016/j.ijleo.2020.165945.

[10] C. Li, J. Huang, K. Wang, Z. Chen, Q. Liu, Optimization of processing parameters of laser skin welding *in vitro* combining the response surface methodology with NSGA- II, *Infrared Physics & Technology*, 2019, **103**, 103067, doi: 10.1016/j.infrared.2019.103067.

[11] M. E. Lou, M. D. Kleinhenz, R. Schroeder, K. Lechtenberg, S. Montgomery, J. F. Coetzee, A. V. Viscardi, Evaluating the utility of a CO_2 surgical laser for piglet tail docking to reduce behavioral and physiological indicators of pain and to improve wound healing: a pilot study, *Applied Animal Behaviour Science*, 2022, **254**, 105720, doi: 10.1016/j.applanim.2022.105720.

[12] A. Priyadarshi, G. K. Keshri, A. Gupta, Dual-NIR wavelength (pulsed 810nm and superpulsed 904nm lasers) photobiomodulation therapy synergistically augments full-thickness burn wound healing: a non-invasive approach, *Journal of Photochemistry and Photobiology B: Biology*, 2023, **246**, 112761, doi: 10.1016/j.jphotobiol.2023.112761.

[13] S. A. Razack, Y. Lee, H. Shin, S. Duraiarasan, B.-S. Chun,

H. W. Kang, Cellulose nanofibrils reinforced chitosan-gelatin based hydrogel loaded with nanoemulsion of oregano essential oil for diabetic wound healing assisted by low level laser therapy, *International Journal of Biological Macromolecules*, 2023, **226**, 220-239, doi: 10.1016/j.ijbiomac.2022.12.003.

[14] P. Wongchadakul, P. Rattanadecho, T. Wessapan, Implementation of a thermomechanical model to simulate laser heating in shrinkage tissue (effects of wavelength, laser irradiation intensity, and irradiation beam area), *International Journal of Thermal Sciences*, 2018, **134**, 321-336, doi: 10.1016/j.ijthermalsci.2018.08.008.

[15] K. Chen, Y. Liang, W. Zhu, X. Sun, T. Wang, Simulation of temperature distribution in skin under laser irradiation with different wavelengths, *Optik*, 2014, **125**, 1676-1679, doi: 10.1016/j.ijleo.2013.10.021.

[16] P. Wongchadakul, Rattanadecho P., Wessapan T, Simulation of temperature distribution in different human skin types exposed to laser irradiation with different wavelengths and laser irradiation intensities, 2019, **41**, 529-538.

[17] J. F. Ready, Effects due to absorption of laser radiation, *Journal of Applied Physics*, 1965, **36**, 462-468, doi: 10.1063/1.1714012.

[18] B.-M. Kim, S. L. Jacques, S. Rastegar, S. Thomsen, M. Motamedi, Nonlinear finite-element analysis of the role of dynamic changes in blood perfusion and optical properties in laser coagulation of tissue, *IEEE Journal of Selected Topics in Quantum Electronics*, 1996, **2**, 922-933, doi: 10.1109/2944.577317.

[19] W.-Z. Liang, P.-F. Liu, E. Fu, H.-S. Chung, C.-R. Jan, C.-H. Wu, C.-W. Shu, Y.-D. Hsieh, Selective cytotoxic effects of low-power laser irradiation on human oral cancer cells, *Lasers in Surgery and Medicine*, 2015, **47**, 756-764, doi: 10.1002/lsm.22419.

[20] S. Koo, S. M. Santoni, B. Z. Gao, C. P. Grigoropoulos, Z. Ma, Laser-assisted biofabrication in tissue engineering and regenerative medicine, *Journal of Materials Research*, 2017, **32**, 128-142, doi: 10.1557/jmr.2016.452.

[21] P. G. Klemens, Heat balance and flow conditions for electron beam and laser welding, *Journal of Applied Physics*, 1976, **47**, 2165-2174, doi: 10.1063/1.322866.

[22] A. Bhowmik, R. Repaka, S. C. Mishra, K. Mitra, Thermal assessment of ablation limit of subsurface tumor during focused ultrasound and laser heating, *Journal of Thermal Science and Engineering Applications*, 2016, **8**, 011012, doi: 10.1115/1.4030731.

[23] S. Wray, M. Cope, D. T. Delpy, J. S. Wyatt, E. O. R. Reynolds, Characterization of the near infrared absorption spectra of cytochrome aa3 and haemoglobin for the non-invasive monitoring of cerebral oxygenation, *Biochimica et Biophysica Acta (BBA) - Bioenergetics*, 1988, **933**, 184-192, doi: 10.1016/0005-2728(88)90069-2.

[24] G. Aguilar, S. H. Díaz, E. J. Lavernia, J. S. Nelson, Cryogen spray cooling efficiency: improvement of port wine stain laser therapy through multiple-intermittent cryogen spurts and laser pulses, *Lasers in Surgery and Medicine*, 2002, **31**, 27-35, doi: 10.1002/lsm.10076.

[25] S.-H. Tseng, P. Bargo, A. Durkin, N. Kollias, Chromophore concentrations, absorption and scattering properties of human skin *in-vivo*, *Optics Express*, 2009, **17**, 14599, doi: 10.1364/oe.17.014599.

[26] R. R. Anderson, J. Hu, J. A. Parrish, Optical radiation transfer in the human skin and applications in *in vivo* remittance spectroscopy. Marks R, Payne PA, Bioengineering and the Skin. Dordrecht: Springer, 1981, 253-265, doi: 10.1007/978-94-009-7310-7_28

[27] H. O. Tabakoglu, N. Topaloglu, M. Gulsoy, The effect of irradiance level in 980-nm diode laser skin welding, *Photomedicine and Laser Surgery*, 2010, **28**, 453-458, doi: 10.1089/pho.2009.2569.

[28] H. H. Pennes, Analysis of tissue and arterial blood temperatures in the resting human forearm, *Journal of Applied Physiology*, 1948, **1**, 93-122, doi: 10.1152/jappl.1948.1.2.93.

[29] A. Welch, The thermal response of laser irradiated tissue, *IEEE Journal of Quantum Electronics*, 1984, **20**, 1471-1481, doi: 10.1109/JQE.1984.1072339.

[30] M. Motamedi, A. Gonzales, G. Yoon, A. J. Welch, Thermal response of gastro-intestinal tissue to Nd-Yag laser irradiation: A theoretical and experimental investigationInternational Congress on Applications of Lasers & Electro-Optics. Los Angeles, California, USA. Laser Institute of America, 1983, doi: 10.2351/1.5057464.

[31] P. Kubelka, New contributions to the optics of intensely light-scattering materials part I, *Journal of the Optical Society of America*, 1948, **38**, 448, doi: 10.1364/josa.38.000448.

[32] A. Kabiri, M. R. Talaee, Thermal field and tissue damage analysis of moving laser in cancer thermal therapy, *Lasers in Medical Science*, 2021, **36**, 583-597, doi: 10.1007/s10103-020-03070-7.

[33] H. E. Cline, T. R. Anthony, Heat treating and melting material with a scanning laser or electron beam, *Journal of Applied Physics*, 1977, **48**, 3895-3900, doi: 10.1063/1.324261.

[34], J. Saemathong, N. Pannucharoenwong, V. Mongkol, S. Vongpradubchai, P. Rattanadecho, Analyzing two laser thermal energy calculation equations: a comparison of beer-lambert's law and light transport equation, *Engineered Science*, 2023, **24**, 912, doi: 10.30919/es912.

